

# Preparation of a hyperbranched polycarbosilane precursor to SiC ceramics following an efficient room-temperature cross-linking process

Zhaoju Yu · Junying Zhan · Muhe Huang · Ran Li ·  
Cong Zhou · Guomei He · Haiping Xia

Received: 3 February 2010 / Accepted: 7 June 2010 / Published online: 16 June 2010  
© Springer Science+Business Media, LLC 2010

**Abstract** Room-temperature cross-linking of a hyperbranched polycarbosilane (HBPCS) with divinylbenzene (DVB) in the presence of the cyclohexanone peroxide–cobaltous naphthenate (CHP–CN) initiator system was studied. According to the Fourier transform infrared spectroscopy (FT-IR) and  $^1\text{H}$  nuclear magnetic resonance ( $^1\text{H}$  NMR) results, the cross-linking reaction occurred via the vinyl polymerization. The GPC analysis confirmed the molecular weight of the cross-linked HBPCS significantly increased. Thermal behaviors of cross-linked HBPCS and original HBPCS were investigated by thermal gravimetric analysis–differential thermal analysis (TGA–DTA). The TGA results indicated that the ceramic yield of HBPCS remarkably increased by the cross-linking treatment. For the HBPCS/10 wt% DVB system, the maximum of reaction degree of HBPCS was obtained, which might be responsible for the highest ceramic yield of 70.1 wt% at 1000 °C. However, the ceramic yield of the non-cross-linked HBPCS was only 45 wt% at 1000 °C. The evolution of crystal structure of SiC as a function of pyrolysis temperature was traced by means of X-ray diffraction (XRD) and FT-IR. With the pyrolysis temperature increasing, the  $\beta$ -SiC peaks became sharper and the grain size also grew larger. As the DVB content increased, the intensity of  $\beta$ -SiC peaks significantly reduced, indicating smaller  $\beta$ -SiC grain size.

## Introduction

As polymers that contain both Si and C in their backbone structure, polycarbosilanes (PCSs) have been of particular interest as precursors to SiC [1], an important high temperature structural ceramic and semiconductor material. Of all the PCSs, liquid hyperbranched PCSs can be regarded as excellent effective precursors especially for a matrix source because of their unique structures and favorable properties [2]. Whitmarsh and Interrante [3] reported the first hyperbranched PCS derived from the Grignard reaction of  $\text{ClCH}_2\text{SiCl}_3$  in ether, yielding a liquid hydridopolycarbosilane (HPCS) with an approximate  $[\text{SiEtH}_{1.85}\text{CH}_2]_n$  compositional formula. An improved preparation of HPCS was subsequently developed by Starfire Systems, Inc., which yields a hyperbranched PCS, namely HBPSE, having an overall  $[\text{SiH}_2\text{CH}_2]_n$  composition [4]. Subsequently, a commercial allyhydridopolycarbosilane (AHPCS) was explored via the introduction of allyl side groups onto the backbone of the HPCS, which was widely studied for its excellent properties as a SiC precursor [5–7]. In our previous work, we successfully synthesized a novel hyperbranched polycarbosilane (HBPCS) by the one-pot synthesis with  $\text{Cl}_3\text{SiCH}_2\text{Cl}$ ,  $\text{Cl}_2\text{Si}(\text{CH}_3)\text{CH}_2\text{Cl}$ , and  $\text{CH}_2=\text{CHCH}_2\text{Cl}$  as the starting materials, and the composition of this HBPCS can be tailored by controlling the amount of the starting materials [8, 9]. The polymer-to-ceramic conversion of the HBPCS for SiC-based ceramics was further studied [10–12].

Polymer crosslinking prior to pyrolysis, conventionally by heating the polymer in atmosphere, is required to increase the ceramic yield [13]. Froehling [14] reported that the final ceramic yield of a branched polyhydridocarbosilane was significantly improved via a previous cross-linking treatment before pyrolysis. As aforementioned HPCS, due to its relatively high cross-linking temperature

Z. Yu · J. Zhan · M. Huang · R. Li · C. Zhou · G. He · H. Xia  
College of Materials, Key Laboratory of High Performance  
Ceramic Fibers (Xiamen University), Ministry of Education,  
Xiamen 361005, China

M. Huang · R. Li · H. Xia (✉)  
College of Chemistry and Chemical Engineering,  
Xiamen University, Xiamen 361005, China  
e-mail: hpxia@xmu.edu.cn

(ca. 300 °C), loss of volatile oligomeric components occurs on unconfined pyrolysis in a flowing nitrogen atmosphere, leading to a ceramic yield of ca. 55% [2, 15]. A detailed study indicated that the main cross-linking mechanism involves the 1,1-elimination of molecular hydrogen from  $\text{SiH}_n$  groups, namely dehydrocoupling, whose rate becomes significant only above ca. 300 °C [16]. It was reported that the enhancement of the ceramic yield of AHPCS, and lowering of the effective cross-linking temperature (to ca. 200 °C), was attributed to the contribution of a thermally induced, intramolecular, hydrosilylation (a reaction between Si–H and vinyl groups) cross-linking [2, 15]. With respect to the HBPCS, we believed that the cross-linking mechanism involved hydrosilylation, dehydrocoupling, and vinyl polymerization, which mainly accounted for the satisfactory ceramic yield [10, 11].

Although the hydrosilylation and the dehydrocoupling reaction were investigated in detail [2, 15, 16], little attention was paid on vinyl polymerization [17]. Our research interests tend to the cross-linking of liquid HBPCS at low temperature via the vinyl polymerization. A conventional redox initiator, namely cyclohexanone peroxide–cobaltous naphthenate (CHP–CN) system was used to initiate the vinyl polymerization based on the foundation that the CHP–CN has been used in the cross-linking of unsaturated polyester resin for over 40 years [18]. Unfortunately, the CHP–CN couple hardly initiated the polymerization of vinyl groups derived from the HBPCS, which might be due to that the allyl groups on Si in HBPCS may not show high reactivity due to the sigma-pi bonding. Therefore, a cross-linking agent rich in vinyl content should be explored to enhance the cross-linking. By far, the hydrosilylation cross-linking of Yajima PCS with divinylbenzene (DVB) as a cross-linking agent has been of great interest due to its obvious improvement in ceramic yield [19]. Also, DVB plays an important role in cross-linking Yajima PCS in the polymer-infiltration-pyrolysis route to prepare fiber-reinforced SiC composites [20–22]. In the present study, DVB was used as the cross-linking agent, improving the cross-linking of HBPCS via vinyl polymerization initiated by CHP–CN initiator system at room temperature. The influence of DVB content on the cross-linking reaction, ceramic yield, and phase composition of the final ceramics were investigated as well.

## Experimental

### Materials

All manipulations involving air and/or water sensitive compounds were performed under nitrogen atmosphere using standard Schlenk technology [23]. HBPCS with a composition

formula  $[\text{SiH}_{1.26}(\text{CH}_3)_{0.60}(\text{CH}_2\text{CH}=\text{CH}_2)_{0.14}\text{CH}_2]_n$  was prepared, as previously described, by a one-pot synthesis with  $\text{Cl}_2\text{Si}(\text{CH}_3)\text{CH}_2\text{Cl}$ ,  $\text{Cl}_3\text{SiCH}_2\text{Cl}$ , and  $\text{CH}_2=\text{CHCH}_2\text{Cl}$  as the starting materials [8, 9]. HBPCS used in this work had a number-average molecular weight of ca. 850 and a polydispersity index of 4.11. Other commercially available reagents were used as received.

### Cross-linking

Cross-linking of HBPCS was carried out in a Schlenk flask with a magnetic stirrer and an argon inlet. A mixture of HBPCS with certain amount DVB was introduced into the Schlenk flask, and then CHP–CN was added to the mixture while being stirred at room temperature (RT) for 12 h in an argon atmosphere. The weight ratio of DVB to HBPCS ranged from 1 to 30 wt%, while the weight ratios of CHP and CN to HBPCS being 2 and 1 wt%, respectively. The liquid HBPCS transformed into a semisolid. These semisolids were used both for TGA and for a macroscopic pyrolysis.

### Pyrolysis

With the pyrolysis temperature ( $T_p$ ) of 900 °C, the uncross-linked or cross-linked sample was put in an alumina boat and heated in a self-made tube furnace in argon flowing at  $200 \text{ cm}^3 \text{ min}^{-1}$ . The temperature was progressively raised up to  $T_p$  at a rate of  $5 \text{ °C min}^{-1}$  and kept at this value for 1 h. For  $T_p > 900 \text{ °C}$ , the sample (pre-pyrolysed at 900 °C) was put in a graphite crucible and heated in a tube furnace (SJG-16, China) with the working temperature range in 1000–1600 °C, in argon flowing at  $200 \text{ cm}^3 \text{ min}^{-1}$ . The pre-pyrolysed sample was heated rapidly to  $T_p$  at a rate of  $40 \text{ °C min}^{-1}$  and kept at this temperature for 10 min.

### Characterization

Fourier transform infrared spectroscopy (FT-IR) spectra were recorded on Nicolet Avator 360 apparatus (Nicolet, Madison, WI) with KBr plates for liquid samples and KBr discs for solid samples.  $^1\text{H}$  nuclear magnetic resonance ( $^1\text{H}$  NMR) experiments were carried out on a Bruker AV300 MHz spectrometer (Bruker, Germany) with  $\text{CDCl}_3$  as a solvent. The  $^1\text{H}$  NMR chemical shifts were all referred to tetramethylsilane (TMS). Gel permeation chromatography (GPC) measurements were performed at 35 °C with tetrahydrofuran (THF) as the eluant ( $1.0 \text{ mL min}^{-1}$ ) using an Agilent 1100 system (Agilent, CA). The spectrum was calibrated with narrow polystyrene standards. Thermal analysis of the samples was carried out on a thermal gravimetric analysis–differential thermal analysis (TGA–DTA) (Netzsch STA 409EP, Netzsch, Germany) in

nitrogen gas with a ramping rate of  $10\text{ }^{\circ}\text{C min}^{-1}$  ranging from room temperature to  $1000\text{ }^{\circ}\text{C}$ . X-ray diffraction (XRD) was carried out by using a PANalytical X'Pert PRO diffractometer (PANalytical, Netherlands) with  $\text{Cu K}\alpha$  radiation. The specimens were continuously scanned from  $10^{\circ}$  to  $90^{\circ}$  ( $2\theta$ ) at a speed of  $0.0167\text{ s}^{-1}$ . The apparent mean grain size of the  $\beta$ -SiC crystalline phase in the sample was calculated from the width of the (111) diffraction peak at mid-height, according to the Scherrer equation [24]. Elemental analyses were carried out by a Horiba Carbon/Sulfur Analyzer EMIA-320V (Horiba, Japan) for carbon element and a Horiba Oxygen Nitrogen Analyzer EMGA-620W (Horiba, Japan) for oxygen element.

## Results and discussion

### Cross-linking

The FT-IR spectra of the original HBPCS, DVB, uncross-linked, and cross-linked HBPCS samples are shown in Fig. 1.

The peaks observed in these spectra were assigned according to the literatures [9–11]. The functional groups in HBPCS including Si-CH<sub>3</sub>, Si-CH<sub>2</sub>-Si, Si-H, and -CH=CH<sub>2</sub> were identified, as followed:  $3076\text{ cm}^{-1}$  (w, C-H stretch in -CH=CH<sub>2</sub>),  $1630\text{ cm}^{-1}$  (w, C=C stretch in -CH=CH<sub>2</sub>),  $2100\text{ cm}^{-1}$  (vs. Si-H stretch),  $940\text{ cm}^{-1}$  (vs. Si-H bending),  $2950$  and  $2873\text{ cm}^{-1}$  (s, CH<sub>3</sub> stretch),  $2920\text{ cm}^{-1}$  (s, CH<sub>2</sub> stretch),  $1400$ ,  $1250\text{ cm}^{-1}$  (Si-CH<sub>3</sub> deformation),  $1355\text{ cm}^{-1}$  (s, Si-CH<sub>2</sub>-Si deformation),

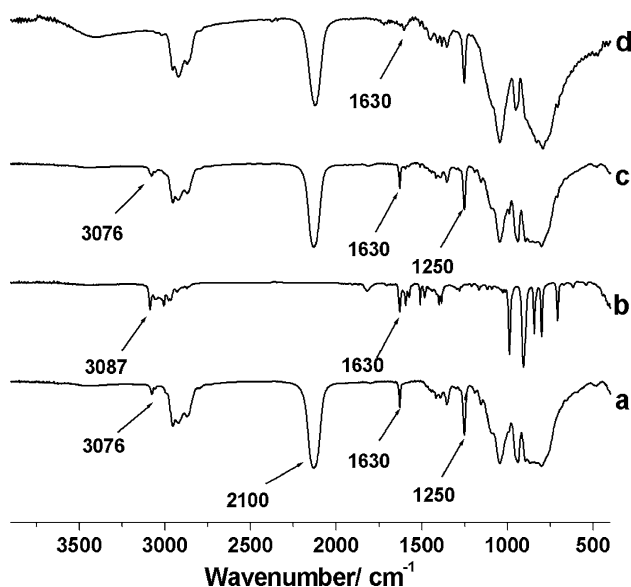


**Fig. 1** FT-IR spectra of (a) original HBPCS, (b) DVB, (c) mixture of HBPCS/10 wt% DVB, and (d) cross-linked HBPCS/10 wt% DVB initiated by CHP-CN initiator system

$1040\text{ cm}^{-1}$  (vs. Si-CH<sub>2</sub>-Si stretch),  $800\text{ cm}^{-1}$  (vs. Si-C stretch). The major peaks significant to DVB were observed at  $3087\text{ cm}^{-1}$  due to C-H stretch in -CH=CH<sub>2</sub> and at  $1630\text{ cm}^{-1}$  due to C=C stretch in -CH=CH<sub>2</sub>. The broadband centered at  $3025\text{ cm}^{-1}$  could be due to phenyl C-H stretching [25]. Other major bonds in DVB indicated were phenyl C-C ( $1594$ ,  $1574\text{ cm}^{-1}$ ), phenyl C-H ( $1510\text{ cm}^{-1}$ ), and phenyl C-C out-of-plane bending ( $900$ – $650\text{ cm}^{-1}$ ). Herein, the intensity ratios of the peaks at  $2100\text{ cm}^{-1}$  (Si-H) and  $1630\text{ cm}^{-1}$  (C=C) to  $1250\text{ cm}^{-1}$  (Si-CH<sub>3</sub>) were denoted as  $A(\text{Si-H})/A(\text{Si-CH}_3)$  and  $A(\text{C=C})/A(\text{Si-CH}_3)$ , respectively. The Si-CH<sub>3</sub> bond should not be involved in the cross-linking reaction at room temperature [19]; hence, the values of  $A(\text{Si-H})/A(\text{Si-CH}_3)$  and  $A(\text{C=C})/A(\text{Si-CH}_3)$  indicate the Si-H and C=C contents. The  $A(\text{C=C})/A(\text{Si-CH}_3)$  values for original HBPCS and the HBPCS/DVB mixture were 0.39 and 0.45, respectively, indicating that the introduction of 10 wt% DVB enhanced the vinyl content. In comparison with uncross-linked mixture, the C=C stretch at  $1630\text{ cm}^{-1}$  obviously reduced in the cross-linked HBPCS. The  $A(\text{C=C})/A(\text{Si-CH}_3)$  for cross-linked sample was 0.11 while a ratio of 0.45 for the non-crosslinked mixture. It seemed that the cross-linking did take place via the consumption of vinyl groups. However, the  $A(\text{Si-H})/A(\text{Si-CH}_3)$  values were 5.71 for the non-crosslinked mixture and 5.67 for the cross-linked sample, indicating that Si-H did not contribute to the cross-linking.

In addition, <sup>1</sup>H NMR spectra of HBPCS, DVB, and cross-linked HBPCS were shown in Fig. 2.

For HBPCS spectrum reported elsewhere [19], the groups of signals around 0 ppm are assigned to the various Si-CH<sub>3</sub> and Si-CH<sub>2</sub> functionalities. The peaks from 3.5 to 4.5 ppm are attributed to Si-H<sub>x</sub> ( $x = 3, 2, \text{ or } 1$ ) protons. The peaks from 1.0 to 2.0 ppm are due to the overlap of methylene protons from THF cleavage and allyl protons from SiCH<sub>2</sub>CH=CH<sub>2</sub>. The two multiples at 4.8 and 5.8 ppm are assigned, respectively, to the protons of SiCH<sub>2</sub>CH=CH<sub>2</sub> and SiCH<sub>2</sub>CH=CH<sub>2</sub>. With respect to DVB <sup>1</sup>H NMR spectrum, the groups of signals around 7.3 ppm are assigned to phenyl protons. The triplet at 6.8 ppm is assigned to vinyl proton from PhCH=CH<sub>2</sub>, and doublets at 5.8 and 5.2 ppm are due to vinyl protons from PhCH=CH<sub>2</sub> [26]. Moreover, three minor peaks from 1 to 3 ppm are observed, due to the methine and methylene protons of DVB oligomer residues [27]. The <sup>1</sup>H NMR spectrum of the cross-linked sample (Fig. 2c) revealed considerably more peaks (1.6 and 7.3 ppm), compared with original HBPCS (Fig. 2a). Importantly, there was an increase in intensity in the peak at 7.3 ppm, suggesting the presence of the aromatic groups of the cross-linking agent in the cross-linked HBPCS. Moreover, the three peaks at 5.2, 5.8, and 6.8 ppm almost disappeared in the cross-linked sample, strongly

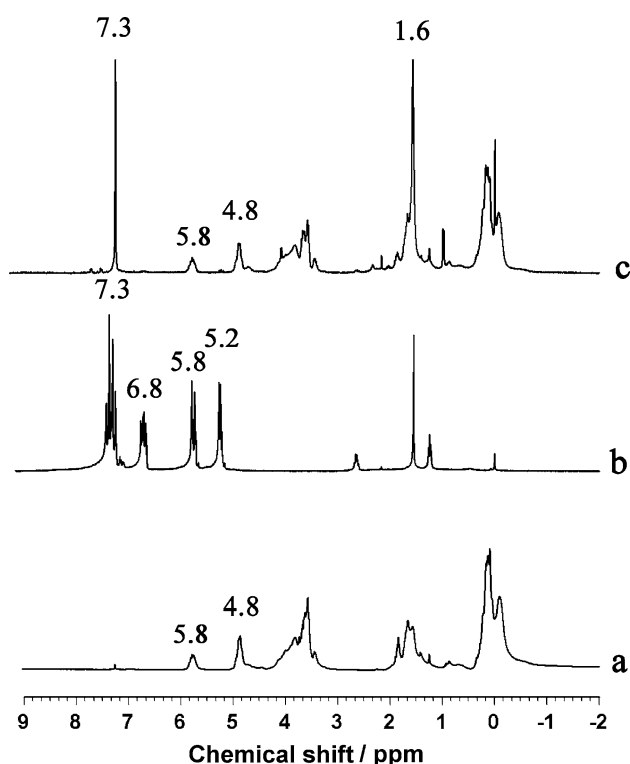


**Fig. 2**  $^1\text{H}$  NMR spectra in  $\text{CDCl}_3$  of (a) original HBPCS, (b) DVB, and (c) cross-linked HBPCS/10 wt% DVB initiated by CHP–CN initiator system

supporting the fact that the vinyl groups of DVB were completely consumed because of vinyl polymerization. The proton signal of main-chain methylenes derived from resultant cross-linked HBPCS appeared at 1.6 ppm, indicating the vinyl polymerization did take place. A blank experiment without DVB was designed, indicating the cross-linking of allyl groups from HBPCS hardly occurred by means of FT-IR and  $^1\text{H}$  NMR. However, allyl groups show improved reactivity when the DVB, as a cross-linking agent, was added. As expected, the intensity in the two peaks at 4.8 and 5.2 ppm reduced obviously, which strongly suggested that some of vinyl groups of HBPCS involved in the cross-linking. In conclusion, the vinyl polymerization between HBPCS and DVB has been confirmed by means of FT-IR and  $^1\text{H}$  NMR.

Subsequently, samples including the original HBPCS, the HBPCS/DVB mixture, and the cross-linked HBPCS were subjected to GPC analysis (Fig. 3). In comparison with the original HBPCS, the molecular weight distribution of the mixture showed an additional sharp peak labeled as  $P_1$ , indicating the GPC curve of DVB. For the cross-linked HBPCS, it was noticeable that the  $P_1$  disappeared while the high molecular weight peaks labeled as  $P_2$ ,  $P_3$ , and  $P_4$  appeared. The results confirmed the molecular mass significantly increased. It was believed that the cross-linking

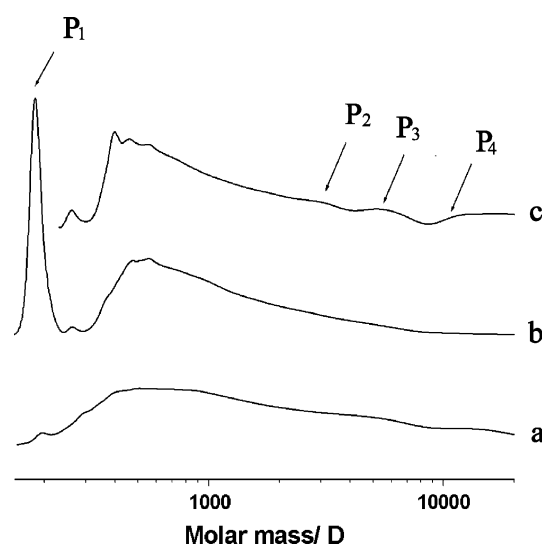


**Fig. 3** GPC traces of (a) original HBPCS, (b) mixture of HBPCS/10 wt% DVB, and (c) cross-linked HBPCS/10 wt% DVB initiated by CHP–CN initiator system

via the vinyl polymerization accounted for the molecular mass increasing.

According to the FT-IR and  $^1\text{H}$  NMR results, the cross-linking reaction of HBPCS initiated by CHP–CN initiator system with DVB as cross-linking agent was given in Fig. 4. Vinyl groups from the DVB and HBPCS copolymerized irregularly to form a network structure. However, the vinyl polymerization hardly occurred without CHP–CN initiator system, by which the initiation effect of CHP–CN on the cross-linking was supported.

As a room temperature initiator system, CHP–CN was widely used in the free radical polymerization, especially in the cross-linking of unsaturated polyester resin [18, 28]. It is well accepted that CHP is the real initiator while CN is the accelerator. The dissociation of CN produces  $\text{Co}^{2+}$  cation, and then  $\text{Co}^{2+}$  accelerates the decomposition of CHP via the redox reaction to give free radicals according to Fig. 5 [28]. Three free radicals were formed, designated as  $R_1$ ,  $R_2$ , and  $R_3$ . Either one of the above radical species can go on and initiate the cross-linking reaction of HBPCS. The cycle is repeated until all CHP is decomposed. Based on the well-known free radical polymerization mechanism [29], the cross-linking reaction involved the copolymerization of HBPCS and DVB initiated by the radical species derived from CHP–CN initiator system (Fig. 5).

#### Thermal behavior

In order to understand the thermal behavior during the pyrolytic conversion of the uncross-linked and cross-linked HBPCS, TGA was measured and shown in Fig. 6.

**Fig. 4** Cross-linking reaction of HBPCS initiated by CHP–CN initiator system with DVB as cross-linking agent

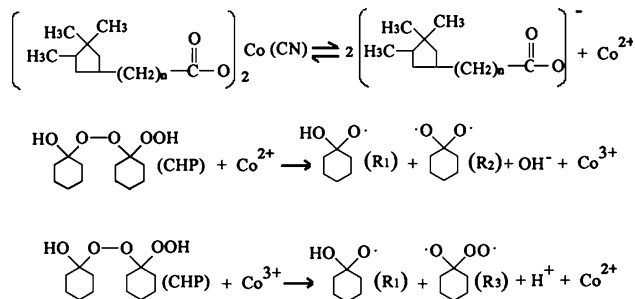
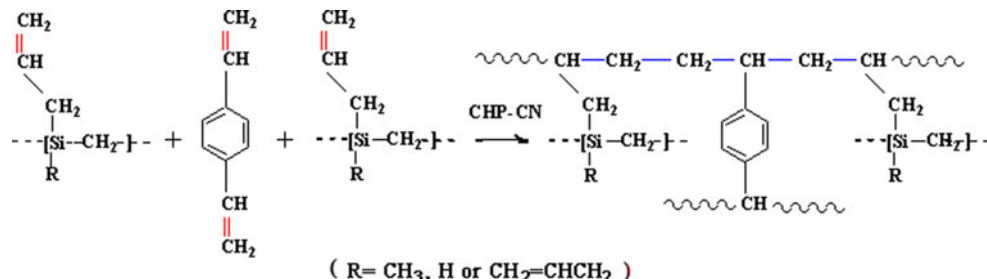


**Fig. 5** Initiation mechanism of CHP–CN initiator system

It was observed that the ceramic yield increased by cross-linking HBPCS prior to polymer pyrolysis. The ceramic yield of cross-linked HBPCS were 68.7, 67.5, 70.1, 65, and 58 wt%, with the addition of 1, 5, 10, 20, and 30 wt% DVB, respectively, while that of the non-crosslinked HBPCS reached only 45 wt% when heated in argon to 1000 °C. However, the ceramic yield increased first and then decreased with increasing DVB concentration, suggesting that only a small amount of crosslinking agent is required to further improve the ceramic yield. The observation is consistent with those of Maddocks et al. [19] due to the decomposition of excessive DVB at high temperatures leading to mass loss, which is supported by that the major mass loss of cross-linked DVB occurred above 380 °C and little mass residue was retained at 1000 °C. It was observed that the obvious weight loss of non-crosslinked sample was 27 wt% between 25 and 400 °C, while that of the cross-linked HBPCS/1 wt% DVB was only 8 wt%. For the 5, 10, 20, and 30 wt% DVB systems, the TGA curves showed the onset of thermal decomposition at ca. 400 °C. It seemed that the significant difference between the non-crosslinked and cross-linked samples was weight loss below 400 °C. It was well-known that hydrogen (H<sub>2</sub>) and methane (CH<sub>4</sub>) are the major volatile species evolved during the pyrolysis of PCS, leading to the mass loss [16, 19]. As reported [16], the evolution rates of H<sub>2</sub> and CH<sub>4</sub> increase rapidly above 425 and 490 °C, respectively. Thus, weight loss below 400 °C was predominately due to the oligomers evaporation. The results suggested that these oligomers were efficiently incorporated into the cross-linked HBPCS, which markedly reduced the evaporation of low-molecular weight

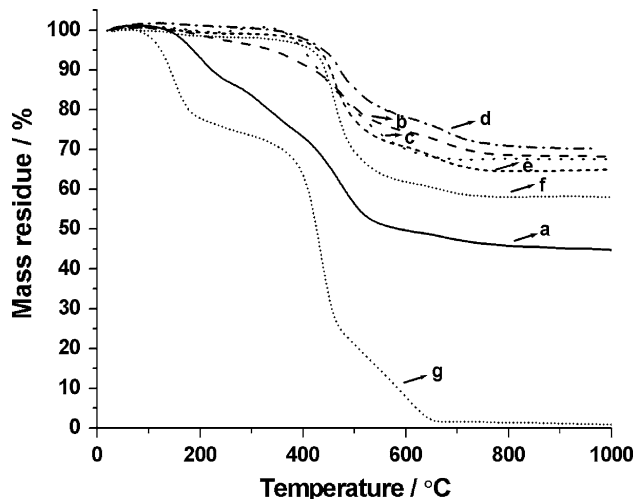


**Fig. 6** TGA curves of (a) original HBPCS and cross-linked HBPCS initiated by CHP–CN with (b) 1 wt% DVB, (c) 5 wt% DVB, (d) 10 wt% DVB, (e) 20 wt% DVB, (f) 30 wt% DVB, and (g) cross-linked DVB

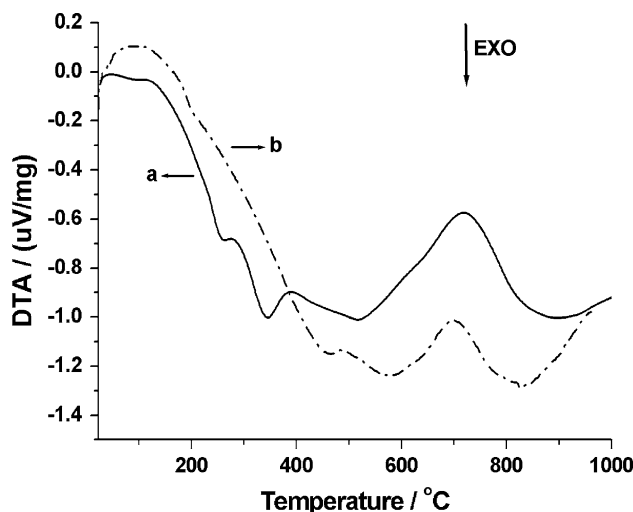


**Fig. 7** DTA curves of (a) original HBPCS and (b) cross-linked HBPCS/10 wt% DVB

oligomers. As a result, higher ceramic yield was gained for the cross-linked samples. In addition, Fig. 7 shows the DTA curves to study the response of cross-linked and uncross-linked HBPCS during thermal treatment. The exothermic

peaks of HBPCS were studied in our previous work [12]. Compared with the DTA curve of HBPCS, it was found that the exothermic peaks of cross-linked HBPCS at about 250 and 360 °C from the hydrosilylation and C=C polymerization almost disappeared. For the cross-linked HBPCS/10 wt% DVB system, the C=C groups were mostly consumed during the cross-linking process, which is responsible for that exothermic phenomena of the hydrosilylation and C=C polymerization became un conspicuous.

Moreover, the ceramic yields of macroscopic pyrolysis at different temperatures were determined and shown in Fig. 8. As expected, the ceramic yields increased first and then decreased with increasing DVB concentration, which is consistent with the TGA results. Under the investigated condition, the optimal weight ratio of DVB to HBPCS is 10 wt% to obtain the highest ceramic yield.

In order to further investigate the effect of amount of DVB on the ceramic yields, the reaction degree of HBPCS during cross-linking process was determined by FT-IR. As mentioned above (Fig. 1), the value of  $A(\text{C}=\text{C})/A(\text{Si}-\text{CH}_3)$  indicates the C=C contents, and the C=C reaction degree ( $P_{\text{C}=\text{C}}$ ) of HBPCS was measured through the characteristic peak's ratios of C=C to Si-CH<sub>3</sub> in FT-IR spectra according to the formula [30]:

$$P_{\text{C}=\text{C}} = \frac{(A_{1630}/A_{1250})_{\text{original}} - (A_{1630}/A_{1250})_{\text{cross-linked}}}{(A_{1630}/A_{1250})_{\text{original}}}$$

The results are shown in Fig. 9. It is worthy mentioning that the  $P_{\text{C}=\text{C}}$  increased first and then decreased with increasing DVB concentration. Obviously, the variation trend of  $P_{\text{C}=\text{C}}$  well agrees with that of the ceramic yields. With the weight ratio of DVB to HBPCS of 10 wt%, the maximum  $P_{\text{C}=\text{C}}$  was gained, indicating the highest the

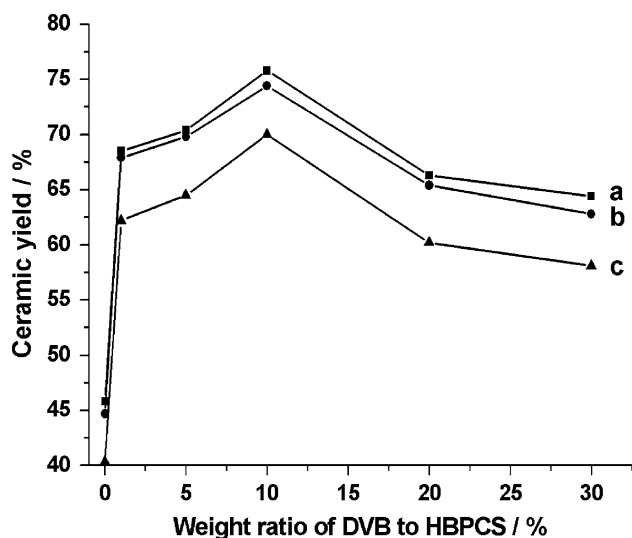


**Fig. 8** Ceramic yields of cross-linked HBPCS and original HBPCS pyrolyzed at (a) 900 °C, (b) 1300 °C, and (c) 1600 °C

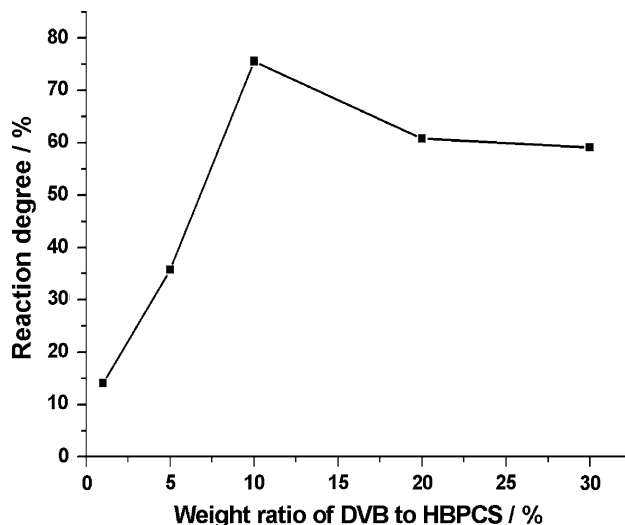


**Fig. 9** Effect of amount of DVB on reaction degree of HBPCS

extent of cross-linking of HBPCS. It is believed that weight gain of the cross-linking and weight loss of pyrolysis are competitive when DVB was involved in the cross-linking reaction. With the DVB feed below 10 wt%, the weight gain of the cross-linking is dominative, leading to increasing of ceramic yield. Otherwise, the weight loss of pyrolysis derived from the decomposition of excessive DVB at high temperatures is dominative with the DVB feed above 10 wt%. As a result, the ceramic yield begins to decrease. For the HBPCS/10 wt% DVB system, the maximum extent of cross-linking was obtained, which might be responsible for the highest ceramic yield.

#### Crystallization behavior

Figure 10 shows the XRD patterns of the pyrolytic residue of cross-linked HBPCS at 900, 1300, and 1600 °C in argon.

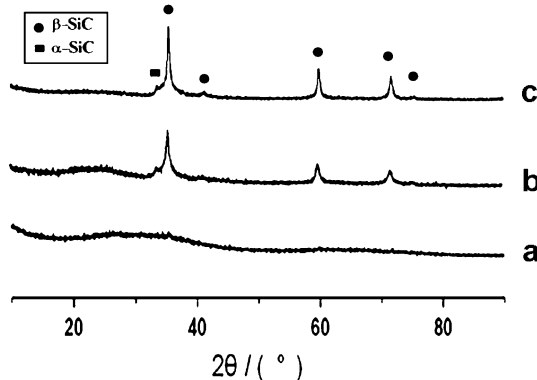


**Fig. 10** XRD patterns of (a) 900 °C, (b) 1300 °C, and (c) 1600 °C ceramics derived from cross-linked HBPCS/20 wt% DVB system

The 900 °C ceramic is amorphous and highly disordered. As the temperature increased, the three major peaks at  $2\theta = 36^\circ$  (111),  $60^\circ$  (220), and  $72^\circ$  (311) appeared, which are attributed to  $\beta$ -SiC [31]. Moreover, the shoulder at  $34^\circ$  is assigned to stacking faults like  $\alpha$ -SiC in  $\beta$ -SiC [32]. The apparent mean grain size of 1300 and 1600 °C ceramics are 12.5 and 15.6 nm, respectively. With the pyrolysis temperature increasing, the  $\beta$ -SiC peaks became sharper and the grain size also grew larger.

The FT-IR spectra of pyrolyzed products at different temperatures are shown in Fig. 11, tracing the evolution of crystal structure of SiC as a function of pyrolysis temperature. At 900 °C, a broad peak centered at about  $780\text{ cm}^{-1}$  was observed, attributed to amorphous SiC framework structure [16]. Further heating to 1300 and 1600 °C led to the sharpening of the SiC band and a shift in its position from 780 to  $800\text{ cm}^{-1}$  at 1300 °C and  $830\text{ cm}^{-1}$  at 1600 °C, consistent with the formation of crystalline SiC [30]. The FT-IR results agree with the XRD well.

The effect of DVB content on the 1600 °C ceramics was also investigated (Fig. 12). The apparent mean grain size of pyrolyzed residues of cross-linked HBPCS with 1, 10, and 20 wt% DVB are 19.0, 18.4, and 15.6 nm, while that of original HBPCS is 26.5 nm. As the DVB content increased, the intensity of  $\beta$ -SiC peaks significantly reduced, indicating smaller  $\beta$ -SiC grain size. For the final ceramics of cross-linked samples, the growth of SiC crystals is inhibited. By referring to the ceramic composition, we find that the higher carbon uptake is responsible by introduction of DVB during cross-linking process. In other words, hetero-elements such as carbon inhibit the growth of SiC crystals, in consistent with the literatures [33, 34].

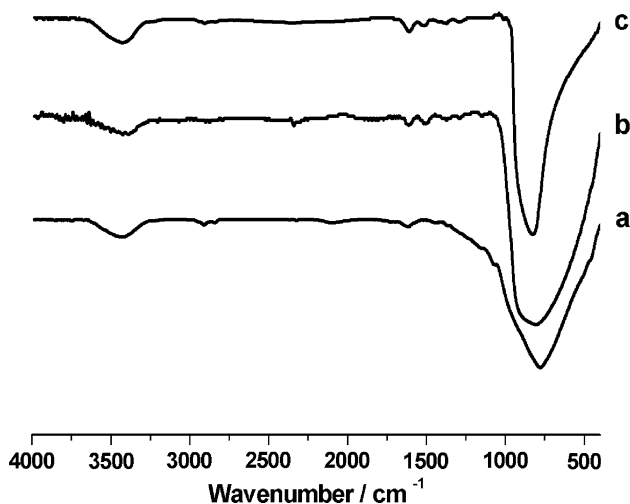


**Fig. 11** FT-IR spectra of (a) 900 °C, (b) 1300 °C, and (c) 1600 °C ceramics derived from cross-linked HBPCS/20 wt% DVB system

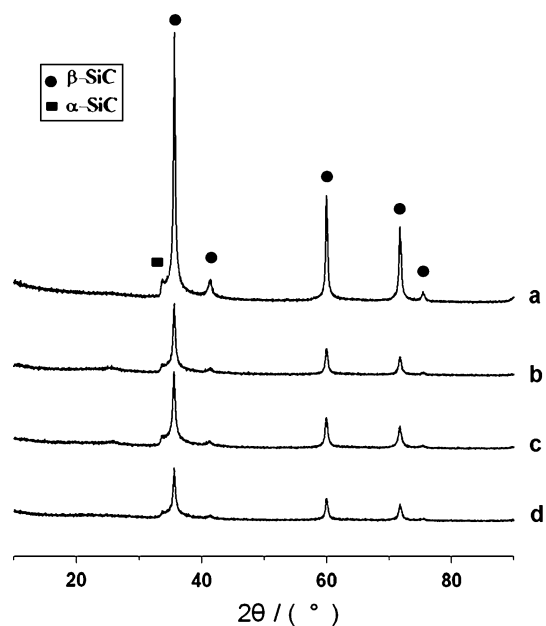


**Fig. 12** XRD patterns of 1600 °C ceramics derived from (a) original HBPCS and cross-linked HBPCS initiated by CHP–CN with (b) 1 wt% DVB, (c) 10 wt% DVB, and (d) 20 wt%

## Conclusions

The cross-linking of HBPCS with DVB in the presence of the CHP–CN initiator system was demonstrated, which was confirmed by means of FT-IR,  $^1\text{H}$  NMR, and GPC. For the cross-linking mechanism, the radical copolymerization of HBPCS and DVB was involved via the vinyl polymerization initiated by radical species derived from CHP–CN initiator system. The TGA results indicated that the ceramic yield of HBPCS remarkably increased by the cross-linking treatment. The cross-linking process markedly reduced the evaporation of low-molecular weight oligomers, which accounted for the difference in the overall ceramic yields between non-crosslinked and cross-linked HBPCS. For the HBPCS/10 wt% DVB system, the maximum of reaction degree of HBPCS was obtained, which might be responsible for the highest ceramic yield of 70.1 wt% at 1000 °C. However, the ceramic yield of the non-crosslinked HBPCS was only 45 wt% at 1000 °C. With the pyrolysis temperature increasing, the  $\beta$ -SiC peaks became sharper and the grain size also grew larger. As the DVB content increased, the intensity of  $\beta$ -SiC peaks significantly reduced, indicating smaller  $\beta$ -SiC grain size.

**Acknowledgements** The project was supported by the National Natural Science Foundation of China (Nos. 50802079, 20925208, and 50532010) and Natural Science Foundation of Fujian Province of China (2008J0165).

## References

1. Kita K, Narisawa M, Nakahira A et al (2010) *J Mater Sci* 45(1):139. doi:[10.1007/s10853-009-3905-x](https://doi.org/10.1007/s10853-009-3905-x)
2. Interrante LV, Shen QH (2009) In: Dvornic PR, Owen MJ (eds) *Silicon-containing dendritic polymers*, chap 12. Springer, Dordrecht
3. Whitmarsh CK, Interrante LV (1991) *Organometallics* 10:1336
4. Rushkin IL, Shen Q, Lehman SE et al (1997) *Macromolecules* 30:3141
5. Interrante LV, Moraes K, MacDonald L et al (2002) *Ceram Trans* 144:125
6. Kotani M, Kato Y, Kohyama A et al (2003) *J Ceram Soc Jpn* 111:300
7. Zheng J, Akinc M (2001) *J Am Ceram Soc* 84:2479
8. Huang TH, Yu ZJ, He XM et al (2007) *Chin Chem Lett* 18:754
9. Huang MH, Fang YH, Li R et al (2009) *J Appl Polym Sci* 113:1611
10. Li HB, Zhang LT, Cheng LF et al (2008) *J Mater Sci* 43:2806. doi:[10.1007/s10853-008-2539-8](https://doi.org/10.1007/s10853-008-2539-8)
11. Li HB, Zhang LT, Cheng LF et al (2008) *J Eur Ceram Soc* 28:887
12. Li HB, Zhang LT, Cheng LF et al (2009) *J Mater Sci* 44:721. doi:[10.1007/s10853-008-3176-y](https://doi.org/10.1007/s10853-008-3176-y)
13. Bouillon E, Pailler R, Naslain R et al (1991) *Chem Mater* 3:356
14. Froehling PE (1993) *J Inorg Organomet Polym* 3:251
15. Interrante LV, Shen QH (2000) In: Jones RG et al (eds) *Silicon-containing polymers*. Kluwer Academic Publishers, Dordrecht
16. Liu Q, Wu HJ, Lewis R et al (1999) *Chem Mater* 11:2038
17. Yu ZJ, Huang MH, Li R et al (2009) *J Chin Ceram Soc* 37:105
18. George SL, Geoffrey P (1969) *I&EC Prod Res Dev* 8:124
19. Maddocks AR, Hook JM, Stender H et al (2008) *J Mater Sci* 43:2666. doi:[10.1007/s10853-008-2488-2](https://doi.org/10.1007/s10853-008-2488-2)
20. Jian K, Chen ZH, Ma QS et al (2007) *Ceram Int* 33:905
21. Jian K, Chen ZH, Ma QS et al (2007) *Ceram Int* 33:73
22. Jian K, Chen ZH, Ma QS et al (2005) *Mater Sci Eng A* 408:330
23. Shriver DF, Drezdson MA (eds) (1986) *The manipulation of air-sensitive compounds*. Wiley, New York
24. Kumagawa K, Yamaoka H, Shibuya M et al (1998) *Ceram Eng Sci Proc* 19:65
25. Zhou MH, Kim SH, Park JG (2000) *Polym Bull* 44:17
26. Ma R, Song ZY, Hou YB et al (2009) *J Macromol Sci A* 46:193
27. Dean JA (ed) (1991) *Lange's chemistry handbook*, 13th edn. Science Press, Beijing
28. Meng GR, Zhao L, Liang GZ et al (2001) *Thermoset Resin* 16: 34 (in Chinese)
29. Michael B, Anton LG (eds) (2001) In: *Macromolecular symposia*. Wiley-VCH, Berlin
30. Yu ZJ, Huang MH, Fang YH et al (2010) *React Funct Polym* 70:334
31. Fang YH, Huang MH, Yu ZJ et al (2008) *J Am Ceram Soc* 91:3298
32. Moraes K, Vosburg J, Wark D et al (2004) *Chem Mater* 16:125
33. Tang M, Yu ZJ, Yu YX et al (2009) *J Mater Sci* 44:1633. doi:[10.1007/s10853-009-3246-9](https://doi.org/10.1007/s10853-009-3246-9)
34. Ogawa I (1997) *Carbon* 35:1846